 MCB, vol.9, no.2, pp.157-173, 2012

Effect of Age-Stiffening Tissues and Intraocular Pressure on Optic Nerve Damages

Leo KK Leung*, **Match WL Ko*** **and David CC Lam**†

Abstract: Age-stiffening of ocular tissues is statistically linked to glaucoma in the elderly. In this study, the effects of age-stiffening on the lamina cribrosa, the primary site of glaucomatous nerve damages, were modeled using computational finite element analysis. We showed that glaucomatous nerve damages and peripheral vision loss behavior can be phenomenologically modeled by shear-based damage criterion. Using this damage criterion, the potential vision loss for 30 years old with mild hypertension of 25mmHg intraocular pressure (IOP) was estimated to be 4%. When the IOP was elevated to 35mmHg, the potential vision loss rose to 45%; and age-stiffening from 35 to 60 years old increased the potential vision loss to 52%. These results showed that while IOP plays a central role in glaucomatous damages, age-stiffening facilitates glaucomatous damages and may be the principal factor that resulted in a higher rate of glaucoma in the elderly than the general population.

Keywords: Glaucoma, damage model, aging model, intraocular pressure, nerve damages

1 Introduction

Optic neuropathy in glaucoma causes visual field loss and blindness [Weinreb, Shakiba, Sample, Shahrokni and VAN (1995); Katz, Gilbert, Quigley and Sommer (1997)]. The optic nerve damages in the lamina cribrosa (LC) of the sclera, the primary site of glaucoma, are correlated with the intraocular pressure (IOP)[Anderson and Hendrickson (1974); Quigley and Addicks (1981); Yan, Coloma, Metheetrairut, Trope, Heathcote and Ethier (1994); Azuara-Blanco, Costa and Wilson

* From the Department of Mechanical Engineering, The Hong Kong University of Science and Technology, Hong Kong, The People's Republic of China

† Corresponding author, The Department of Mechanical Engineering, The Hong Kong University of Science and Technology, Clear Water Bay, Hong Kong; Email: david.lam@ust.hk; Tel no.: (+852) 23588661

(2002)]. The linkage between IOP and glaucoma has been investigated using computational models [Sigal, Flanagan, Tertinegg and Ethier (2004); Burgoyne, Crawford Downs, Bellezza, Francis Suh and Hart (2005); Sigal, Flanagan and Ethier (2005); Sigal, Flanagan, Tertinegg and Ethier (2009); Sigal, Flanagan, Tertinegg and Ethier (2009)]. In general, the tangential tensile strains are correlated with IOP. Eyes with high scleral stiffness were predicted to have lower strains at the LC and the optic nerve head (ONH)[Sigal, Flanagan and Ethier (2005)]. However, these computational results were at odds with the clinical observation that age-stiffened eyes in the elderly [Friberg and Lace (1988); Pallikaris, Kymionis, Ginis, Kounis and Tsilimbaris (2005); Hommer, Fuchsjager-Mayrl, Resch, Vass, Garhofer and Schmetterer (2008); Girard, Suh, Bottlang, Burgoyne and Downs (2009)] suffer more nerve damages, not less [Quigley (1996)]. Moreover, experimental studies showed that the optic nerves are sheared at high IOP [Yan, Coloma, Metheetrairut, Trope, Heathcote and Ethier (1994)]. Since glaucomatous vision loss starts from the periphery, a phenomenologically consistent model should also show that damages start at the periphery. In this study, we will show that the damage progression can be modeled using a shear-based approach.

After the establishment of the phenomenologically consistency, the relation between the ocular stiffness and shear stresses in the LC was quantitatively studied. The finite element analysis will show that the age-stiffening is an important contributing factor in progressive vision loss.

2 Methods

A 3-dimensional human eyeball model (Figure 1)was built in a computer-aided design (CAD) software (Solidworks 2007, DassaultSystemesSolidworks Corp.), and imported to a finite element analysis (FEA) software (ANSYS Simulation 11.0, SP1, ANSYS, Inc.) for computational simulation. The core structural dimensions (Figure 1) of the globe and ONH, such as the internal radius of eyeball shell, the scleral thickness and the LC thickness were adapted from Sigal's study[Sigal, Flanagan and Ethier (2005)]. The eye with adipose tissue was assumed to be axisymmetric about the central axis of the LC. The adipose tissue was set to cover 140 degrees of the eye, and the thickness of the adipose tissues was set to 4.6mm. The LC anterior surface central deflection (LCCD) was assumed to be 0.1mm. The central corneal thickness, corneal diameter and radius of curvature of the cornea were 0.5mm, 11mm and 7.8mm, respectively. The disc diameter was set to be 1.8mm, and a cup-to-disc diameter ratio (CDR)[Heidelberg Engineering GmbH)]of 0.45 was used.The shape and the dimensions of the pre-laminar neural tissue were adapted from Sigal[Sigal, Flanagan and Ethier (2005)]and are shown in Table 1. Since the blind spot is ˜15 degrees nasally from the fovea [Allingham, Shields,

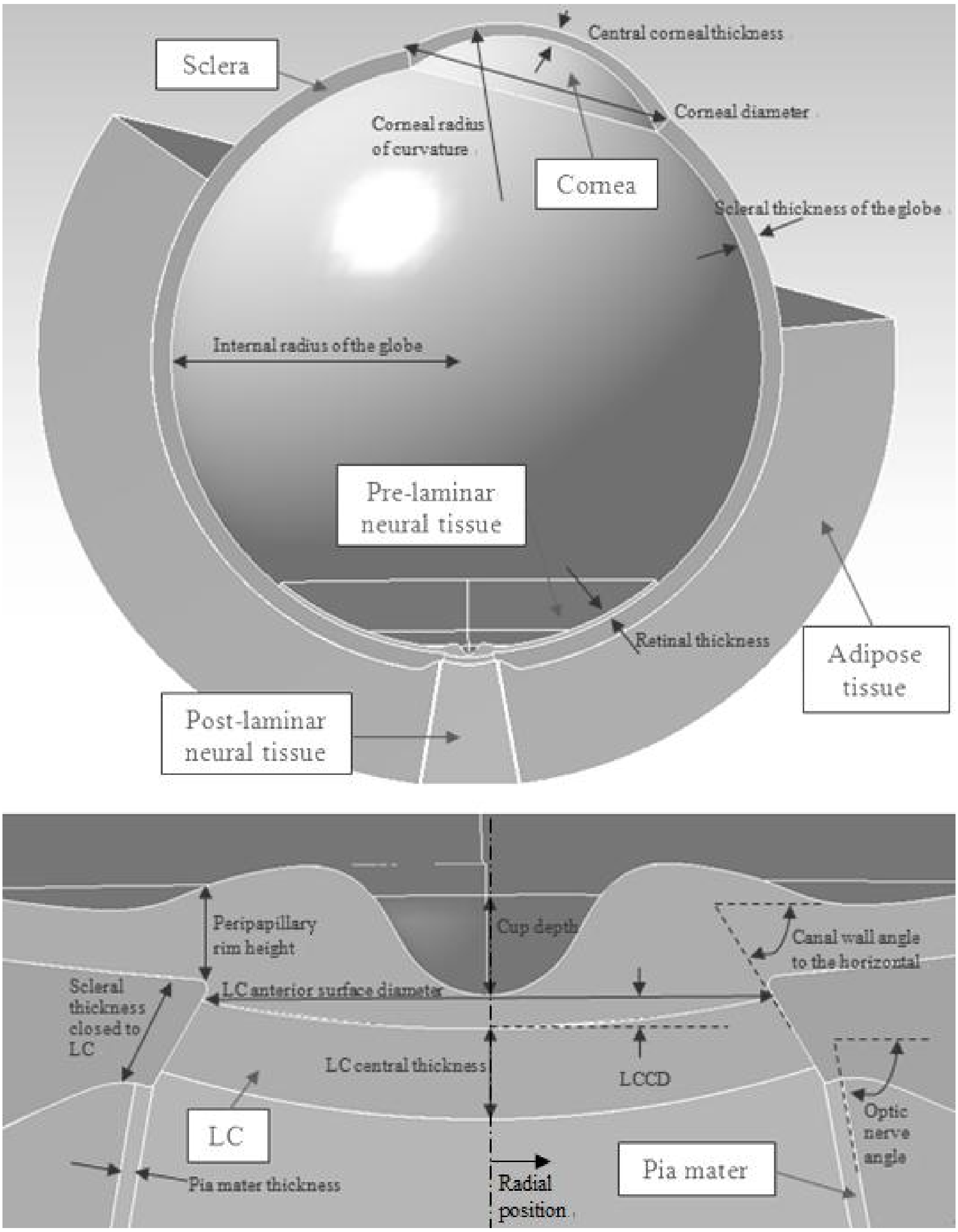

Figure 1: FEM model used in this study. The dimensions and material properties of tissues are detailed in Methods and Table 1.

Damji, Freedman, Moroi and Shafranov (2005)], the 165^o angle between the central axis of cornea and that of the ONH region was used. Since variation in the coverage angle of the pre-laminar neural tissue does not affect significantly the deformation within the ONH region, the coverage angle of the pre-laminar neural tissue was set at 80^o.

The baseline material properties used in our model are shown inTable 1. The baseline elastic moduli of sclera, LC, retina, optic nerve and diameter were the same as those used by Sigal's group [Sigal, Flanagan and Ethier (2005)], and the elastic modulus of cornea was adapted from the paper by Hamilton [Hamilton and Pye (2008)]. The elastic modulus of the adipose tissue attached to the globe was approximated as the same as that of the soft tissue in human buttocks [Todd and Thacker (1994); Bidar, Ragan, Kernozek and Matheson (2000); Power (2001)].To examine the effects of tissue stiffness, the scleral elastic modulus, E_s, was varied from 1 to 9 MPa and the elastic modulus of the lamina cribrosa, E_{LC}, was varied from 0.1 to 0.9MPa [Sigal, Flanagan and Ethier (2005)].

The intraocular pressure exerted on the inner surface of the pre-laminar neural tissue, the sclera and the cornea by the vitreous body of the eye was simulated by applying normal pressure loads evenly onto the inner surfaces of the eye. Coarse meshing of the structure was auto-generated by the FEA software. The mesh in the ONH region was manually refined until the outputs has <0.5% differences even when the mesh density was doubled. The numerical accuracy was comparable to the Sigal's study[Sigal, Flanagan and Ethier (2005)].

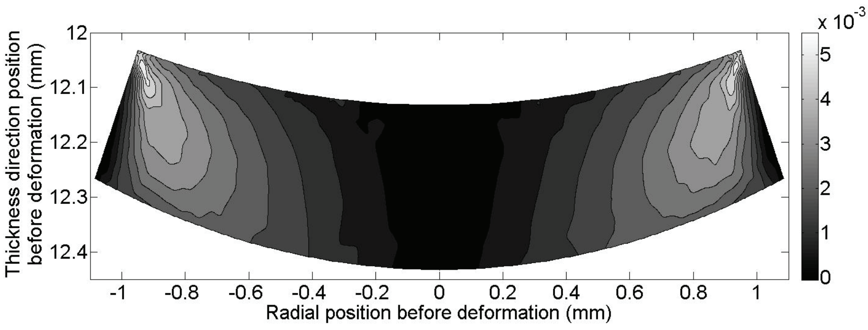

Figure 2: Effect of elevated IOP on shear stresses in the LC: Shear stress distribution in the diametrical cross-section of the LC for the case of IOP=25mmHg, E_s=3MPa and E_{LC}=0.3MPa is shown.The radial position is as defined inFigure 1.

Table 1: Summary of the geometric parameters, material properties and mechanical loading in the eyeball FEM model used in this study.

Name	**Unit**	**Baseline value**	**Sources/ References**
Internal radius of the globe	mm	12.0	[Sigal, Flanagan and Ethier (2005)]
Scleral thickness of the globe	mm	0.8	[Sigal, Flanagan and Ethier (2005)]
Scleral thickness closed to LC	mm	0.4	[Sigal, Flanagan and Ethier (2005)]
LC central thickness	mm	0.3	[Sigal, Flanagan and Ethier (2005)]
Retinal thickness	mm	0.2	[Sigal, Flanagan and Ethier (2005)]
LC anterior surface diameter	mm	1.9	[Sigal, Flanagan and Ethier (2005)]
Central corneal thickness	mm	0.5	[Ren, Wang, Li, Li, Gao, Xu and Jonas (2009)]
Corneal diameter	mm	11	[Ren, Wang, Li, Li, Gao, Xu and Jonas (2009)]
Corneal radius of curvature	mm	7.8	[Bier and Lowther (1977); Orssengo and Pye (1999)]
Pia mater thickness	mm	0.06	[Sigal, Flanagan and Ethier (2005)]
LCCD	mm	0.10	[Sigal, Flanagan and Ethier (2005)]
Canal wall angle to the horizontal	deg	60	[Sigal, Flanagan and Ethier (2005)]
Optic nerve angle	deg	80	[Sigal, Flanagan and Ethier (2005)]
CDR	–	0.45	[Sing, Noelani, Anderson and Townsend (2000)]
Cup depth	mm	0.33	[Sigal, Flanagan and Ethier (2005)]
Peripapillary rim height	mm	0.3	[Sigal, Flanagan and Ethier (2005)]
IOP	mmHg	25	[Sigal, Flanagan and Ethier (2005)]
Poisson ratio of all material	–	0.49	[Sigal, Flanagan and Ethier (2005)]
Elastic modulus of adipose tissue	MPa	0.047	[Todd and Thacker (1994); Bidar, Ragan, Kernozek and Matheson (2000); Power (2001)]
Elastic modulus of cornea	MPa	0.29	[Hamilton and Pye (2008)]
Elastic modulus of pia mater	MPa	3	[Sigal, Flanagan and Ethier (2005)]
Elastic modulus of prelaminar neural tissue	MPa	0.03	[Sigal, Flanagan and Ethier (2005)]
Elastic modulus of postlaminar neural tissue	MPa	0.03	[Sigal, Flanagan and Ethier (2005)]

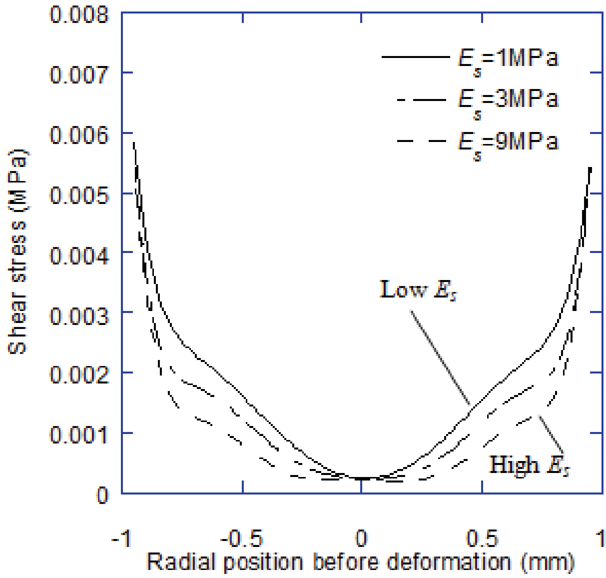

Figure 3: Effect of E_s on shear stresses in the LC: Shear stress distribution on the anterior surface of the LC as a function of radial position of the LC for different E_s, with fixed E_{LC}=0.3MPa and constant IOP=25mmHg.

3 Results

Glaucomatous vision loss starts at the periphery and progresses toward the center [Drance (1972); Allingham, Shields, Damji, Freedman, Moroi and Shafranov (2005)]. Since the damaged nerves are shown to be sheared [Yan, Coloma, Metheetrairut, Trope, Heathcote and Ethier (1994); Edwards, Steven and Good (2008)], shear stresses from the computational model should be higher at the periphery and lower at the center of the LC. The local maximum shear stresses in the LC from our baseline modelat 25mmHg are shown in Figure 2. The results showed that the local maximum shear stresses were highest at the peripheral anterior surface and lowest in the central anterior surface. The effect of tissue stiffness on the shear stresses is plotted in Figure 3 and Figure 4. The data showed that LC stiffening (Figure 4) increased the stresses in the LC, while scleral stiffening (Figure 3) lowered the shear stresses. When both tissues were stiffened together (Figure 5), the shear stresses increased.

The overall average stress behavior in the tissue is shown in Figure 6. When both the sclera and the LC were stiffened together (solid triangles), the average shear

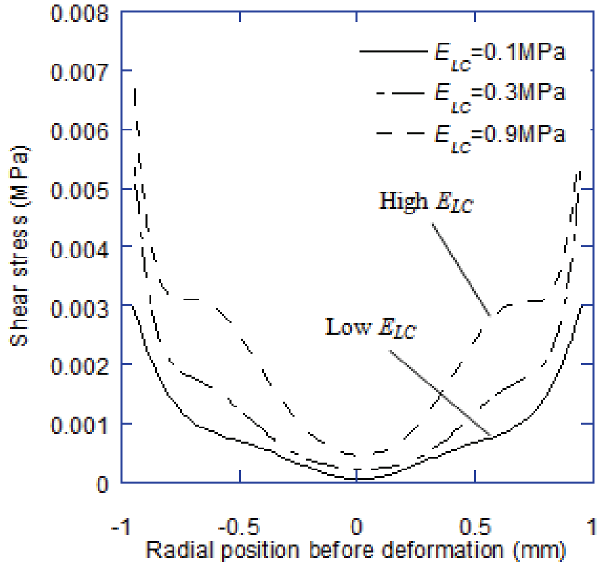

Figure 4: Effect of E_{LC} on shear stresses in the LC: Shear stress distribution on the anterior surface of the LC against radial position of the LC for different E_{LC} , with fixed E_s=3MPa and constant IOP=25mmHg.

stress in the LC increased. When the LC and scleral tissue effects are examined independently, the plot showed that the global average shear stress in the LC decreased with scleral stiffening, but the entire curve shifted upward when the LC was stiffened. This suggests that both the the average shear stress and the top anterior shear stress in the LC are dominated by the LC itself. Since the LC and the sclera stiffen with age[Friberg and Lace (1988); Albon, Purslow, Karwatowski and Easty (2000)], aging would increase the shear stresses in the LC even when IOP is unchanged.

3.1 Effect of aging

Glaucomatous vision loss is positively correlated with IOP and age. The elastic properties of the ocular tissues are also linearly correlated with IOP [Albon, Purslow, Karwatowski and Easty (2000); Girard, Suh, Bottlang, Burgoyne and Downs (2009)](Figure 7) and nonlinearly correlated with age (Figure 8 and Figure 9) [Friberg and Lace (1988); Albon, Purslow, Karwatowski and Easty (2000); Sigal, Flanagan and Ethier (2005)]. On the basis of the plots, E_s and E_{LC} for the

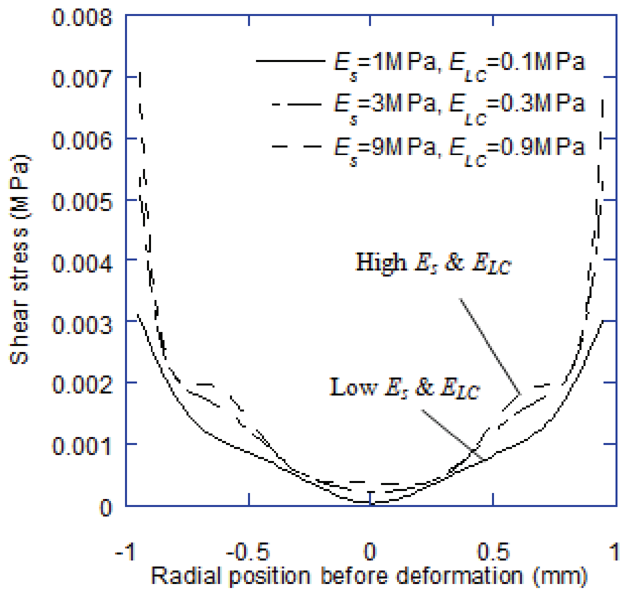

Figure 5: Effect of co-stiffening of E_s and E_{LC} on the shear stresses in the LC: Shear stress distribution on anterior surface of the LC against radial position of the LC for co-stiffening of E_s and E_{LC} at constant IOP=25mmHg.

sclera and the LC at different age and IOP are interpolated from the plots and used in the model.

For vision loss, the classical Tresca shear failure criterion (maximum shear stress failure criterion) [Tresca (1864); Gardiner and Weiss (2001); Yu (2004); Ionescu, Guilkey, Berzins, Kirby and Weiss (2006)] was adopted. Vision is classified as lost when $\tau_a \geq \tau_c$, i.e., when τ_a, the shear stress in a nerve fiber along the thickness direction, exceeded τ_c, the Tresca critical damage shear stress.

$\tau_{\max}$, the maximum shear stresses along the thickness direction in the LC were determined from the model. Statistically, damage is negligible in normal eyes. To satisfy this boundary condition, τ_c was taken as 0.0035MPa in the simulations such that $\tau_{\max}$ in normal eyes (E_s=1MPa and E_{LC}=0.1MPa) under mild ocular hypertension (IOP = 25mmHg) does not exceed τ_c. Using the criterion, the damages for normal eye were estimated and are shown in Figure 10. The results showed that nerve damages increased with tissue stiffening. Using the correlations established in Figure 8 and Figure 9, the damages as a function of age are plotted in Figure 11. The plot showed the people with IOP less than 25mmHg have less than 30%

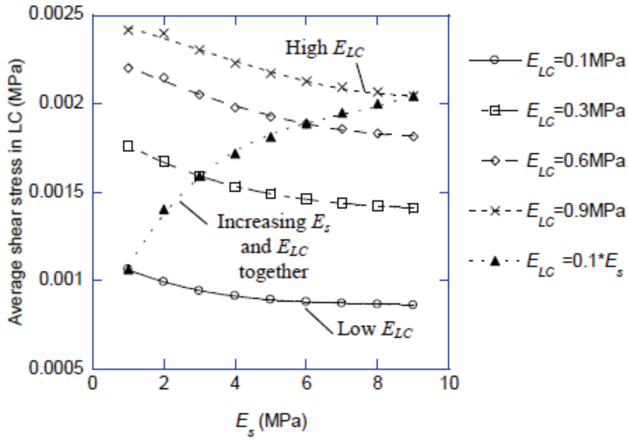

Figure 6: Effects of the sclera and LC on shear stresses in the LC: Average shear stress in the LC against E_s for different E_{LC} at constant IOP=25mmHg.

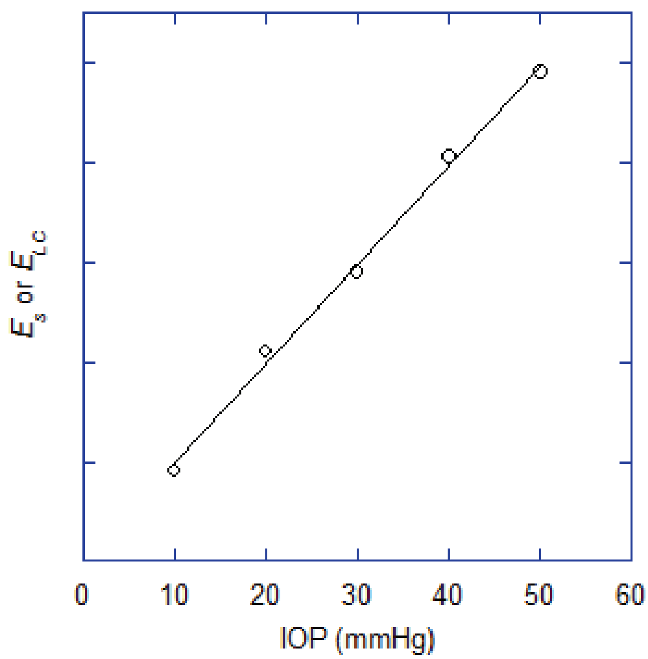

Figure 7: Schematic diagram showing the IOP dependence of E_s and E_{LC}.

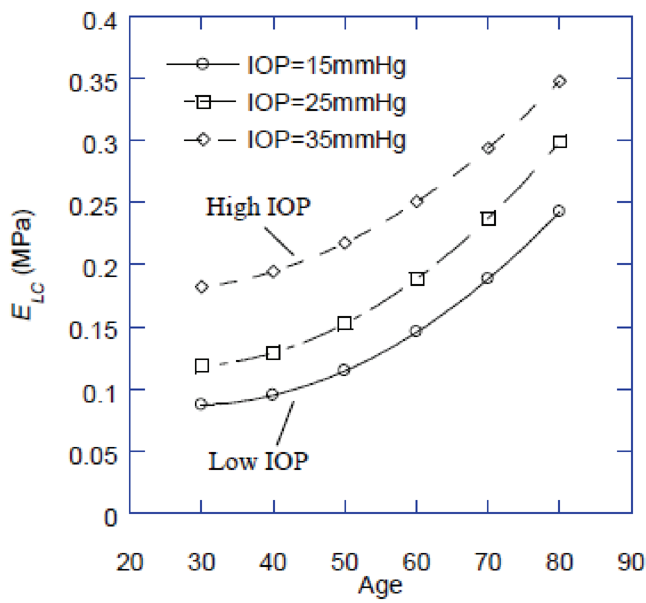

Figure 8: E_{LC} as a function of age and IOP. The age-dependence of E_{LC} was taken from the age-stiffness trend reported by Albon[Albon, Purslow, Karwatowski and Easty (2000)] and reference E_{LC} was taken to be 0.1MPa at IOP being 22mmHg and age 30. The E_{LC}were in the range of the material data used by Sigal [Sigal, Flanagan and Ethier (2005)].

damages, and normal age-stiffening in the elderly resulted only in minor vision loss. Since the majority of the general population do not have optic nerve damages and glaucoma [Kingman (2004)], the simulation results are in line with population trend.

On the other hand, Figure 12 showed that people with inherently higher ocular tissue stiffnesses suffered 25% to >135% more damages depending on IOP. This means that the elderlies with age-stiffened ocular tissues are more susceptible to IOP-induced nerve damages compared to younger people.

4 Discussions

The shear stress-based model successfully explained the general observation that glaucomatous vision loss often starts from the periphery. When used together with the Tresca failure criterion, we showed that age-stiffened eyes are more sensitive to nerve damages from elevated IOP. The results from this study showed that the nerve

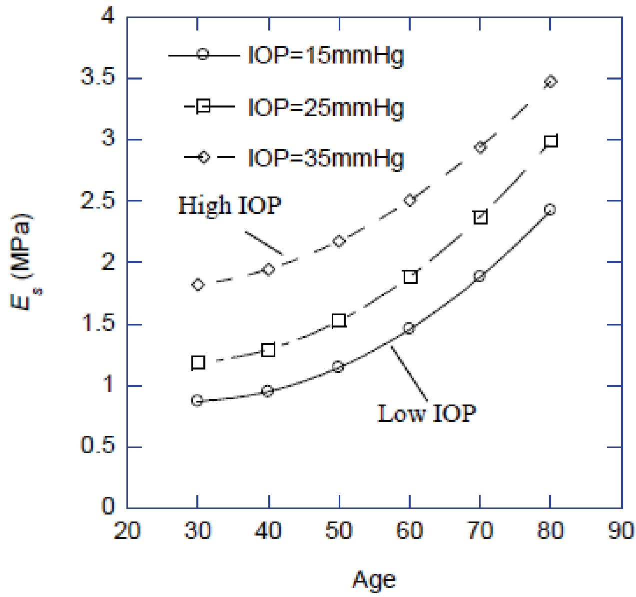

Figure 9: E_s as a function of age and IOP using the same age-dependence shown in Figure 8 and reference E_s was taken to be 1MPa at IOP being 22mmHg and age 30. The E_s were in the range of the experimental data from Friberg [Friberg and Lace (1988)] and material data used by Sigal [Sigal, Flanagan and Ethier (2005)].

damages from IOP are amplified by high ocular tissue stiffness, but high ocular stiffness itself does not cause nerve damages. The results also showed that age-stiffened eye are undamaged if IOP is normal. This is in line with the observed trend that the majority of the elderly has normal IOP do not suffer from glaucoma. For the population of people with age-stiffened eyes, the results showed that they are more sensitive to nerve damages from elevated IOP. These are people with higher risk and should be monitored more frequently than people with normal ocular stiffnesses. To identify the people at high risk, methods can be developed to characterize the *in vivo* ocular tissue stiffness.

5 Remarks

The foregoing analysis was developed on the basis of the results from the simplified eye model used in this study. In real eyes, the intraocular pressure is not a constant, but varies in a 24-hour cycle and the properties are generally viscoelastic and its behaviors are time-dependent. In most computational models of the eye,

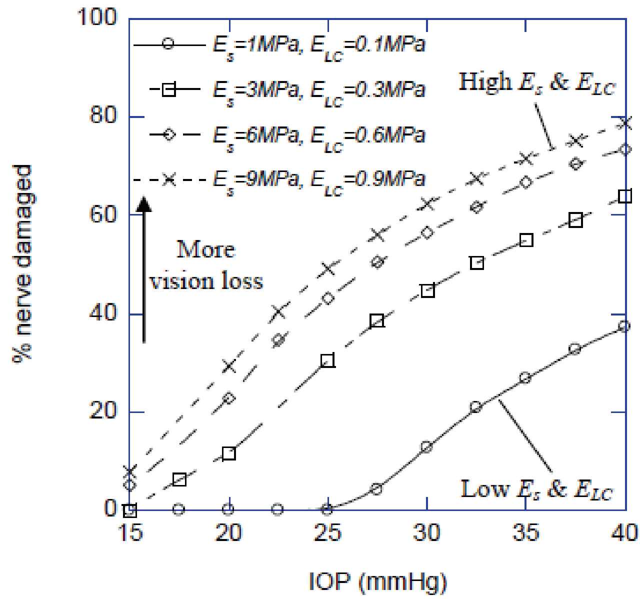

Figure 10: Effect of simultaneous increase in E_s and E_{LC} on nerve damages:Percentage nerve damaged (for $\tau_c = 0.0035$MPa) against IOP for different E_s and E_{LC}.

these complex features were generally ignored because their inclusion requires further assumptions about the viscoelastic material laws and material parameters that govern them. With already a long list of parameters in the model, the inclusion of more parameters may not lead to better understanding of the eye behavior, but more confusion. By recognizing the pitfalls of complex models, we have chosen to add only two essential elements into the shear-focused model, i.e., age-dependence and damage criterion, while following the linear elastic modeling approach used in the literature[Sigal, Flanagan, Tertinegg and Ethier (2004); Burgoyne, Crawford Downs, Bellezza, Francis Suh and Hart (2005); Sigal, Flanagan and Ethier (2005); Sigal, Flanagan, Tertinegg and Ethier (2009); Sigal, Flanagan, Tertinegg and Ethier (2009)]. Both elements were added with reference to the real behaviors and checked against the clinical trends. The age-dependence of the sclera was developed from experimental data. Comparison showed that the relation is in good agreement with reported data. The second element added was the nerve damage criterion. Since the experimental evidence indicated that the nerves were damaged by shear[Yan, Coloma, Metheetrairut, Trope, Heathcote and Ethier (1994); Edwards, Steven and Good (2008)], the classical criterion for shear stress, the single param-

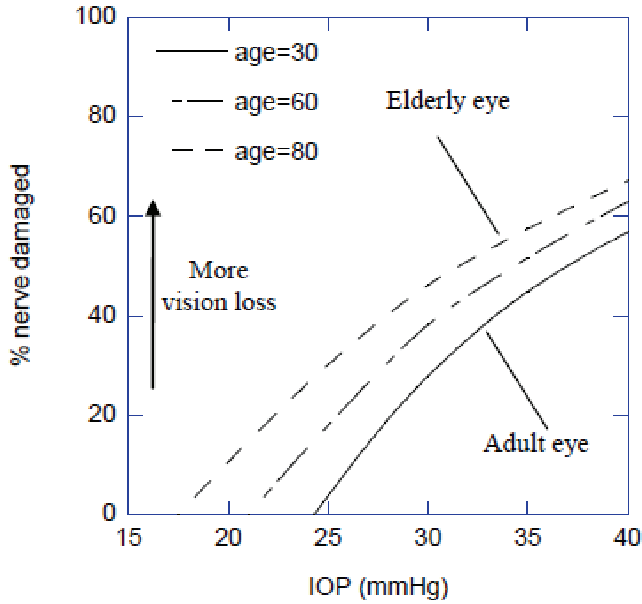

Figure 11: Effect of aging on nerve damages in normal eyes: Percentage nerve damaged (for $\tau_c = 0.0035$MPa) as a function of IOP at different ages for normal population. The E_s and E_{LC} used in the model were interpolated from the data in Figure 8 and Figure 9.

eter Tresca shear failure criterion was borrowed from classical failure mechanics [Tresca (1864); Gardiner and Weiss (2001); Yu (2004); Ionescu, Guilkey, Berzins, Kirby and Weiss (2006)] and adopted as the initial criterion for nerve damages. A crucial test of the criterion is not only whether the criterion predicted nerve damages at high IOP, but minimal damages when IOP is low. Computational results in this study showed that the Tresca criterion reasonably predicted the behavior. More complex damage models that account for potential dependence on age, anisotropic behavior of nerve fibers and time dependence can be added, but as a first criterion, the Tresca criterion appears to be sufficient since it modeled observed behavior. Refinement can be incorporated when clinical data on age-dependence are available.

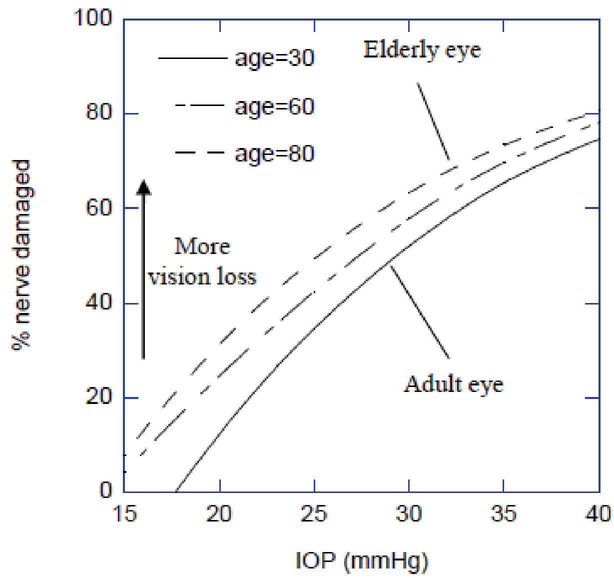

Figure 12: Effect of aging on nerve damages in inherently stiffened eyes: Percentage nerve damaged (for $\tau_c = 0.0035$MPa) against IOP at different ages for tripled E_s and E_{LC} of that in Figure 8 and Figure 9.

6 Conclusions

Optic nerve damages from high IOP can be reasonably characterized by shear-based Tresca criterion. The study showed that shear stresses in the LC are higher in eyes with stiffened ocular tissues subjected to the same IOP. Consequently, in addition to IOP, the ocular stiffness of the eye should also be measured *in vivo* to identify high risk glaucoma patients for alternate aggressive treatment and to arrest vision loss. Further clinical studies are needed to examine the potential use of ocular stiffness in glaucoma risk screening to identify patients at high risk of glaucoma.

References

1. Albon, J., Purslow, P. P., Karwatowski, W. S. S. and Easty, D. L. (2000): Age related compliance of the lamina cribrosa in human eyes. *British Journal of Ophthalmology* 84(3): 318.

2. Allingham, R. R., Shields, M. B., Damji, K. F., Freedman, S., Moroi, S. E. and Shafranov, G. (2005): Shields' textbook of glaucoma, Lippincott Williams & Wilkins.

3. Anderson, D. R. and Hendrickson, A. (1974): Effect of intraocular pressure on rapid axoplasmic transport in monkey optic nerve. *Investigative ophthalmology & visual science* 13(10): 771.

4. Azuara-Blanco, A., Costa, V. P. and Wilson, R. P. (2002): Handbook of glaucoma, Informa HealthCare.

5. Bidar, M., Ragan, R., Kernozek, T. and Matheson, J. W. (2000): Finite element calculation of seat-interface pressures for various wheelchair cushion thicknesses. *Chicago, Illinois*.

6. Bier, N. and Lowther, G. (1977): Contact lens correction, Butterworth-Heinemann.

7. Burgoyne, C. F., Crawford Downs, J., Bellezza, A. J., Francis Suh, J. K. and Hart, R. T. (2005): The optic nerve head as a biomechanical structure: a new paradigm for understanding the role of IOP-related stress and strain in the pathophysiology of glaucomatous optic nerve head damage. *Progress in retinal and eye research* 24(1): 39-73.

8. Drance, S. M. (1972): The glaucomatous visual field. *British Medical Journal* 56(3): 186.

9. Edwards, M. E., Steven, S. S. W. and Good, T. A. (2008): Role of viscoelastic properties of differentiated SH-SY5Y human neuroblastoma cells in cyclic shear stress injury. *Biotechnology progress* 17(4): 760-767.

10. Friberg, T. R. and Lace, J. W. (1988): A comparison of the elastic properties of human choroid and sclera. *Experimental Eye Research* 47(3): 429-436.

11. Gardiner, J. C. and Weiss, J. A. (2001): Simple shear testing of parallel-fibered planar soft tissues. *Journal of biomechanical engineering* 123: 170.

12. Girard, M. J. A., Suh, J. K., Bottlang, M., Burgoyne, C. F. and Downs, J. C. (2009): Scleral Biomechanics in the Aging Monkey Eye. *Investigative ophthalmology & visual science*.

13. Girard, M. J. A., Suh, J. K. F., Bottlang, M., Burgoyne, C. F. and Downs, J. C. (2009): Scleral biomechanics in the aging monkey eye. *Investigative ophthalmology & visual science* 50(11): 5226-5237.

14. Hamilton, K. E. and Pye, D. C. (2008): Young's modulus in normal corneas and the effect on applanation tonometry. *Optometry & Vision Science* 85(6): 445.

15. Heidelberg Engineering GmbH: Quantitative Three-Dimensional Imaging of the Posterior Segment with the Heidelberg Retina Tomograph.

16. Hommer, A., Fuchsjager-Mayrl, G., Resch, H., Vass, C., Garhofer, G. and Schmetterer, L. (2008): Estimation of ocular rigidity based on measurement of pulse amplitude using pneumotonometry and fundus pulse using laser interferometry in glaucoma. *Investigative ophthalmology & visual science* 49(9): 4046.

17. Ionescu, I., Guilkey, J. E., Berzins, M., Kirby, R. M. and Weiss, J. A. (2006): Simulation of soft tissue failure using the material point method. *Journal of biomechanical engineering* 128: 917.

18. Katz, J., Gilbert, D., Quigley, H. A. and Sommer, A. (1997): Estimating progression of visual field loss in glaucoma. *Ophthalmology* 104(6): 1017-1025.

19. Kingman, S. (2004): Glaucoma is second leading cause of blindness globally. *Bulletin of the World Health Organization* 82: 887-888.

20. Orssengo, G. and Pye, D. (1999): Determination of the true intraocular pressure and modulus of elasticity of the human cornea in vivo. *Bulletin of mathematical biology* 61(3): 551-572.

21. Pallikaris, I., Kymionis, G., Ginis, H., Kounis, G. and Tsilimbaris, M. (2005): Ocular rigidity in living human eyes. *Investigative ophthalmology & visual science* 46(2): 409.

22. Power, E. D. (2001): A nonlinear finite element model of the human eye to investigate ocular injuries from night vision goggles.

23. Quigley, H. (1996): Number of people with glaucoma worldwide. *British Medical Journal* 80(5): 389.

24. Quigley, H. A. and Addicks, E. M. (1981): Regional differences in the structure of the lamina cribrosa and their relation to glaucomatous optic nerve damage. *Archives of ophthalmology* 99(1): 137.

25. Ren, R., Wang, N., Li, B., Li, L., Gao, F., Xu, X. and Jonas, J. (2009): Lamina cribrosa and peripapillary sclera histomorphometry in normal and

advanced glaucomatous Chinese eyes with various axial length. *Investigative ophthalmology & visual science* 50(5): 2175.

26. Sigal, I. A., Flanagan, J. G. and Ethier, C. R. (2005): Factors influencing optic nerve head biomechanics. *Investigative ophthalmology & visual science* 46(11): 4189.
27. Sigal, I. A., Flanagan, J. G., Tertinegg, I. and Ethier, C. R. (2004): Finite element modeling of optic nerve head biomechanics. *Investigative ophthalmology & visual science* 45(12): 4378.
28. Sigal, I. A., Flanagan, J. G., Tertinegg, I. and Ethier, C. R. (2009): Modeling individual-specific human optic nerve head biomechanics. Part I: IOP-induced deformations and influence of geometry. *Biomechanics and modeling in mechanobiology* 8(2): 85-98.
29. Sigal, I. A., Flanagan, J. G., Tertinegg, I. and Ethier, C. R. (2009): Modeling individual-specific human optic nerve head biomechanics. Part II: influence of material properties. *Biomechanics and modeling in mechanobiology* 8(2): 99-109.
30. Sing, T., Noelani, M., Anderson, S. and Townsend, J. (2000): The normal optic nerve head. *Optometry & Vision Science* 77(6): 293.
31. Todd, B. A. and Thacker, J. G. (1994): Three-dimensional computer model of the human buttocks, in vivo. *Journal of Rehabilitation Research and Development* 31: 111-111.
32. Tresca, H. E. (1864): Memoire sur l'ecoulement des corps solides soumis a de fortes pressions, Gauthier-Villars.
33. Weinreb, R. N., Shakiba, S., Sample, P. A., Shahrokni, S. and VAN, H. (1995): Association between quantitative nerve fiber layer measurement and visual field loss in glaucoma. *American journal of ophthalmology* 120(6): 732-738.
34. Yan, D. B., Coloma, F. M., Metheetrairut, A., Trope, G. E., Heathcote, J. G. and Ethier, C. R. (1994): Deformation of the lamina cribrosa by elevated intraocular pressure. *British Journal of Ophthalmology* 78(8): 643.
35. Yu, M. (2004): Unified strength theory and its applications, Springer.